Critical parameters of the three-dimensional Ising spin glass

M. Baity-Jesi,[1,2,3] R. A. Baños,[3,4] A. Cruz,[4,3] L.A. Fernandez,[1,3] J. M. Gil-Narvion,[3] A. Gordillo-Guerrero,[5,3] D. Iñiguez,[3,6] A. Maiorano,[2,3] F. Mantovani,[7] E. Marinari,[8] V. Martin-Mayor,[1,3] J. Monforte-Garcia,[3,4] A. Muñoz Sudupe,[1] D. Navarro,[9] G. Parisi,[8] S. Perez-Gaviro,[3,6] M. Pivanti,[7] F. Ricci-Tersenghi,[8] J. J. Ruiz-Lorenzo,[10,3] S.F. Schifano,[11] B. Seoane,[2,3] A. Tarancon,[4,3] R. Tripiccione,[7] and D. Yllanes[2,3]

[1]*Departamento de Física Teórica I, Universidad Complutense, 28040 Madrid, Spain.*
[2]*Dipartimento di Fisica, La Sapienza Università di Roma, 00185 Roma, Italy.*
[3]*Instituto de Biocomputación y Física de Sistemas Complejos (BIFI), 50009 Zaragoza, Spain.*
[4]*Departamento de Física Teórica, Universidad de Zaragoza, 50009 Zaragoza, Spain.*
[5]*D. de Ingeniería Eléctrica, Electrónica y Automática, U. de Extremadura, 10071, Cáceres, Spain.*
[6]*Fundación ARAID, Diputación General de Aragón, Zaragoza, Spain.*
[7]*Dipartimento di Fisica e Scienze della Terra, Università di Ferrara, and INFN, Ferrara, Italy.*
[8]*Dipartimento di Fisica, IPCF-CNR, UOS Roma Kerberos and INFN, La Sapienza Università di Roma, 00185 Roma, Italy.*
[9]*D. de Ingeniería, Electrónica y Comunicaciones and I3A, U. de Zaragoza, 50018 Zaragoza, Spain.*
[10]*Departamento de Física, Universidad de Extremadura, 06071 Badajoz, Spain.*
[11]*Dipartimento di Matematica e Informatica, Università di Ferrara and INFN, Ferrara, Italy*

We report a high-precision finite-size scaling study of the critical behavior of the three-dimensional Ising Edwards-Anderson model (the Ising spin glass). We have thermalized lattices up to $L = 40$ using the Janus dedicated computer. Our analysis takes into account leading-order corrections to scaling. We obtain $T_c = 1.1019(29)$ for the critical temperature, $\nu = 2.562(42)$ for the thermal exponent, $\eta = -0.3900(36)$ for the anomalous dimension and $\omega = 1.12(10)$ for the exponent of the leading corrections to scaling. Standard (hyper)scaling relations yield $\alpha = -5.69(13)$, $\beta = 0.782(10)$ and $\gamma = 6.13(11)$. We also compute several universal quantities at T_c.

PACS numbers: 75.50.Lk, 75.40.Mg

I. INTRODUCTION

Spin glasses are disordered magnetic alloys whose understanding has defied physicists for decades.[1,2] In this context, the Ising Edwards-Anderson model[3] has played a major role. However, in spite of its prominence, it took 25 years to show that it undergoes a continuous phase transition at a critical temperature T_c[4,5] (there was an earlier consensus on the existence of a phase transition,[6–11] but its nature had remained unclear). Amusingly, evidence for a phase transition on experimental spin glasses had been obtained several years before.[12]

Since then, the critical behavior of the Edwards-Anderson model has been studied numerically in a number of papers.[13–24] In these works, microscopic details such as the distribution of the coupling constants differ. It was unclear whether universality violations were present in the problem because the critical exponents and other universal quantities seemed to depend on those microscopic details (although some authors[19,21,25] argued that these apparent violations were caused by corrections to scaling). The issue was settled in 2008 by Hasenbusch, Pelissetto and Vicari,[24] who emphasized the role of corrections to scaling, thus convincing the community that universality holds. Furthermore, their computation of most universal quantities is still the most accurate to date.

Here we present a high-precision finite-size scaling study of the Ising Edwards-Anderson model. Using the Janus special-purpose computer,[26,27] we thermalize the largest lattices to date ($L = 40$), with a very large number of samples. Even with this increased accuracy, we confirm that the analysis with leading-order scaling corrections is adequate (however, see below Sect. V B). In this way, we achieve a determination of the critical exponents four times more accurate than the one in Ref. 24. We also compute a number of universal quantities not previously considered in the literature. Reliable determinations of the critical parameters are important to make progress in other fronts, such as the study of the correlation functions below T_c,[28] or the behavior of spin glasses in an externally applied magnetic field.[29,30]

The organization of the remaining part of this work is as follows. In Section II A we define the model and provide details about our simulations. The quantities that we compute are defined in Section II B. The finite-size scaling analysis is briefly reviewed in Section III. Our main results are given in Section IV, where we compute the critical exponents, including the corrections to scaling exponent ω (see also Appendix A), as well as the critical correlation length in units of the lattice size ξ_L/L and the Binder cumulant U_4. With this input, we proceed to compute in Section V other universal cumulants and the critical temperature. Finally, we discuss our conclusions in Section VI. For ease of reference our main results are summarized in Table I.

II. MODEL, SIMULATIONS, OBSERVABLES

A. Model and simulations

We consider Ising spins $s_{\boldsymbol{x}} = \pm 1$, defined on the $V = L^D$ nodes of a cubic lattice of linear size L and spatial dimension $D = 3$, with periodic boundary conditions. The interactions in the Hamiltonian H are restricted to lattice nearest neighbors:

$$H = -\sum_{\langle \boldsymbol{x},\boldsymbol{y}\rangle} J_{\boldsymbol{x},\boldsymbol{y}} s_{\boldsymbol{x}} s_{\boldsymbol{y}} \,. \tag{1}$$

Quantity	Source
$\omega = 1.12(10)$	Joint fit
$\eta = -0.3900(36)$	
$\nu = 2.562(42)$	
$R^*_\xi = 0.6516(32)$	
$U^*_4 = 1.4899(28)$	
$\alpha = -5.69(13)$	Derived quantities
$\beta = 0.782(10)$	
$\gamma = 6.13(11)$	
$T_c = 1.1019(29)$	Secondary fits
$U^*_{1111} = 0.4714(14)$	
$U^*_{22} = 0.7681(16)$	
$U^*_{111} = 0.4489(15)$	
$B^*_\chi = 2.4142(51)$	
$R^*_{12} = 2.211 \pm 0.006$	

TABLE I. Summary of our results for the universality class of the Ising spin glass (see definitions in Sect. II B). The first block of five quantities comes from a joint fit reported in Fig. 2 and Sect. IV. The second block of quantities includes the remaining critical exponents, which can be derived from ν and η (taking correlations into account for the errors). The third block of quantities come from secondary individual fits. The computation of the critical temperature T_c is reported in Fig. 3 and Sect. V A. Finally, the remaining universal quantities are computed in Sect. V B. In all cases we have employed the quotients method and performed fits with leading corrections to scaling for all data with $L \geq L_{\min} = 8$. Since we computed all the covariance matrices from $O(10^3)$ jackknife blocks, our error estimates are significant beyond the first digit. The error for R^*_{12} is of a systematic nature (rather than statistical, see Sect. V B).

L	N_{samples}	$N^{\min}_{\text{MCS}}$	$N^{\max}_{\text{MCS}}$	N_{T}	$T_{\min}$	$T_{\max}$
6	8 192 000	40 000	40 000	10	1.100	1.703
8	8 192 000	80 000	80 000	10	1.100	1.703
10	8 192 000	80 000	80 000	10	1.100	1.703
12	8 192 000	80 000	80 000	14	1.100	1.651
16	1 024 000	800 000	800 000	14	1.100	1.651
20	768 000	1 600 000	1 600 000	14	1.100	1.651
24	512 000	3 200 000	3 200 000	23	1.100	1.626
32	256 000	1 600 000	99 200 000	22	1.100	1.600
40	48 000	6 400 000	204 800 000	28	1.100	1.594

TABLE II. Details of the simulations. We show the simulation parameters for each lattice size L. N_{samples} is the number of simulated samples. N_{T} is the number of temperatures that were used in parallel tempering. In the set of temperatures we always include the values 1.1, 1.11266, 1.12532, 1.13797, and evenly space the remaining $N_{\text{T}} - 4$ temperatures up to $T_{\max}$ (the temperature resolution was increased near T_c in order to ease interpolations). The number of temperatures N_{T} was chosen so that the parallel tempering's acceptance was at least of 15%. $N^{\min}_{\text{MCS}}$ is the minimum number of Monte Carlo steps (MCS) in each simulation. Each MCS consisted of 10 Metropolis (heat-bath in $L = 32, 40$) full-lattice sweeps, followed by a parallel-tempering temperature swap. In the larger lattices ($L = 32$, 40) we extend the simulation of specific samples after measuring the exponential correlation time.[33] The average simulation time was larger than the minimal one by a factor 1.6 ($L = 32$) or 1.4 ($L = 40$).

The coupling constants $J_{\boldsymbol{x},\boldsymbol{y}}$ can take the two values ± 1 with 50% probability. We study quenched disorder, meaning that the $J_{\boldsymbol{x},\boldsymbol{y}}$ cannot change with time (see, e.g., Ref. 2). Each instance of the $\{J_{\boldsymbol{x},\boldsymbol{y}}\}$ is called *sample*. For any quantity of interest O, we first compute the thermal average $\langle O \rangle$ and only afterwards we take the average over the different samples $\overline{\langle O \rangle}$.

For every sample we simulate four real replicas $\{s^a_{\boldsymbol{x}}\}$, $a = 1, 2, 3$ and 4. All four replicas share the same set of coupling constants $\{J_{\boldsymbol{x},\boldsymbol{y}}\}$, but they are otherwise statistically independent.

We employ parallel tempering.[31,32] We simulate lattices of size up to $L = 24$ on the *Memento* CPU cluster at BIFI. Multi-spin coding with streaming extensions allows us to simulate 128 samples in parallel. On the other hand, lattices of linear sizes $L = 32$ and 40 are simulated on Janus. The main features of our simulations are reported in Table II. As a whole, the simulations on *Memento* for lattice sizes $L \leq 24$ implied a total of 2.99×10^{19} Metropolis spin updates (the equivalent of 1.33×10^5 days of a single core of the machine). The simulations on Janus ($L = 32, 40$) consisted of a total of 5.03×10^{19} heat-bath spin updates, equivalent to about 27 400 days of a single processing unit (FPGA).

We have checked that our data are not affected by thermalization effects. For the largest lattice sizes ($L = 32, 40$) we use the method reported in Ref. 33, which consists in computing the exponential autocorrelation time τ_{exp} for each sample, using the temperature random walk during the parallel tempering. We extend each sample until the simulation time is at least $16\tau_{\text{exp}}$ (therefore, the length of the simulation depends on the sample, as shown on Table II). For the lattices simulated with multi-spin coding, this sample-by-sample method is more involved.[29] Therefore, taking into account that almost all our observables are measured during the simulation, we have decided to use the more traditional approach of studying the time evolution of sample-averaged quantities on a logarithmic scale. All the quantities that we have considered are stable on the last two logarithmic bins, corresponding to the second half and the second quarter of the run. In fact, this condition is satisfied even if we subtract from each successive bin the result over the last half of the measurements, thus significantly reducing the error bars.[34]

In general, we compute all the physical quantities by averaging over the second half of the simulation. However, as a further check, we have also recomputed all the final quantities using only the last block of measurements (which, depending on the lattice, corresponds from 6% to 25% of the total simulation time). We find no differences greater than one fifth of a standard deviation (which, in any case, corresponds to the increase in the statistical error of thermal averages).

B. Observables

The main quantities are computed in terms of the overlap field

$$q^{ab}_{\boldsymbol{x}} = s^a_{\boldsymbol{x}} s^b_{\boldsymbol{x}} \,. \tag{2}$$

Its spatial correlation function is

$$G(\boldsymbol{r}) = \frac{1}{V}\sum_{\boldsymbol{x}} \overline{\langle q^{ab}_{\boldsymbol{x}+\boldsymbol{r}} q^{ab}_{\boldsymbol{x}}\rangle}\,, \tag{3}$$

while the spin-glass order parameter is the spatial average

$$q^{ab} = \frac{1}{V}\sum_{\boldsymbol{x}} q^{ab}_{\boldsymbol{x}}\,. \tag{4}$$

The reader will notice that, having four replicas at our disposal, there are six equivalent ways of choosing the pair of replica indices ab. We shall merely write q to imply that we average over all possible replica index combinations in order to improve our statistics.

The second-moment correlation length is computed from the Fourier transform of the correlation function

$$\chi(\boldsymbol{k}) = \frac{1}{V}\sum_{\boldsymbol{r}} G(\boldsymbol{r})\, e^{i\boldsymbol{k}\cdot\boldsymbol{r}}\,. \tag{5}$$

Specifically,[35,36]

$$\xi = \frac{1}{2\sin(k_{\rm min}/2)}\sqrt{\frac{\chi(0)}{\chi(\boldsymbol{k}_{\rm min})} - 1}, \tag{6}$$

where $\boldsymbol{k}_{\rm min} = (2\pi/L, 0, 0)$ or permutations. We remark as well that the spin-glass susceptibility is

$$\chi_{\rm SG} = \chi(0) = V\overline{\langle q^2\rangle}\,. \tag{7}$$

We shall often study the correlation length in units of the system size

$$R_\xi = \xi/L, \tag{8}$$

whose value is universal at the critical point.

It will be useful to consider six more dimensionless quantities, which are also universal at $T_{\rm c}$:

$$U_4 = \frac{\overline{\langle q^4\rangle}}{\overline{\langle q^2\rangle}^2}\,, \tag{9}$$

$$U_{22} = \frac{\overline{\langle q^2\rangle^2}}{\overline{\langle q^4\rangle}}\,, \tag{10}$$

$$U_{111} = \frac{\overline{\langle q^{12} q^{23} q^{31}\rangle}^{4/3}}{\overline{\langle q^4\rangle}}\,, \tag{11}$$

$$U_{1111} = \frac{\overline{\langle q^{12} q^{23} q^{34} q^{41}\rangle}}{\overline{\langle q^4\rangle}}\,, \tag{12}$$

$$R_{12} = \frac{\chi(2\pi/L, 0, 0)}{\chi(2\pi/L, 2\pi/L, 0)}, \tag{13}$$

$$B_\chi = 3V^2\frac{\overline{\langle|\hat{q}(2\pi/L, 0, 0)|^4\rangle}}{[\chi(2\pi/L, 0, 0)]^2}\,, \tag{14}$$

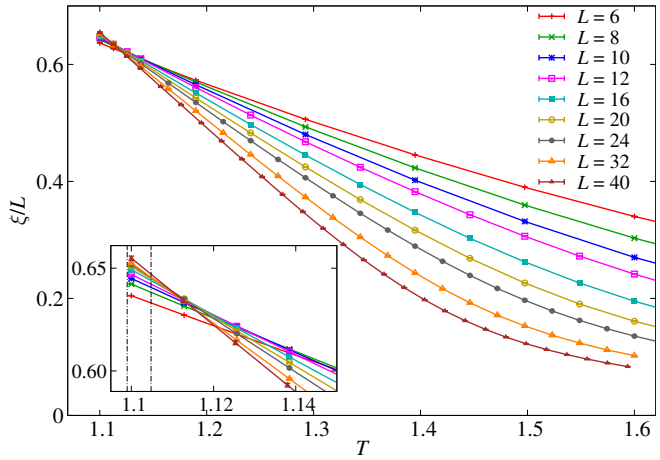

FIG. 1. (color online). Plot of the second-moment correlation length ξ, Eq. (6), in units of the lattice size L for all our simulated systems as a function of temperature. The inset is a detailed view of the critical region, showing scale invariance, where the vertical lines mark our final estimate for (the error interval of) the critical temperature, $T_{\rm c} = 1.1019(29)$.

where

$$\hat{q}^{ab}(\boldsymbol{k}) = \frac{1}{V}\sum_{\boldsymbol{x}} q^{ab}_{\boldsymbol{x}}\, e^{i\boldsymbol{k}\cdot\boldsymbol{x}}\,. \tag{15}$$

In order to gain statistics, we average over all equivalent wavevectors in Eqs. (13) and (14). Similarly, we average over all the equivalent choices for the replica indices in Eqs. (11) and (12). We recall that R_{12} was crucial to understand the critical behavior in a magnetic field.[29] Some of the other quantities have been studied before.[37]

Temperature derivatives are computed in two ways. We either use the connected correlations with the energy, or we perform a third-order polynomial interpolation and differentiate it. We have found that both determinations differ only in a small fraction of the error bars (which were computed using the jackknife method, see, e.g., Ref. 36). In our final results, we have employed the interpolation-polynomial method.

III. FINITE-SIZE SCALING ANALYSIS

To extract the value of critical points, critical exponents and dimensionless quantities, we employ the quotients method,[36,38,39] also known as phenomenological renormalization. This method allows a particularly transparent study of corrections to scaling. Previous applications to disordered systems include diluted ferromagnets,[40] spin glasses[5,19,25,41–45] and systems belonging to the random-field Ising model realm.[46–48]

The method is actually very simple. We compare observables computed in pairs of lattices $(L, 2L)$. We start by imposing scale invariance. We look for the L-dependent critical point: the value of T such that $\xi_{2L}/\xi_L = 2$ (i.e., the *crossing* point for $R_\xi = \xi_L/L$, see Fig 1).

Now, for dimensionful quantities O, which scale as $\xi^{x_O/\nu}$ in the thermodynamical limit, we consider the quotient $Q_O = O_{2L}/O_L$ at the crossing. Instead, for dimensionless quantities g the ratio g_{2L}/g_L trivially goes to one, therefore we focus on g_L. In either case, one has:

$$Q_O^{\rm cross} = 2^{x_O/\nu} + O(L^{-\omega})\,,\ g_L^{\rm cross} = g^* + O(L^{-\omega})\,, \qquad (16)$$

where x_O/ν, g^* and the scaling-corrections exponent ω are universal. Examples of dimensionless quantities are R_ξ, the six cumulants defined in Eqs. (9–13). Instances of dimensionful quantities are the temperature derivatives of ξ ($x_{\partial_T \xi} = 1+\nu$), the temperature derivatives of each of the six cumulants ($x_{\partial_T g} = 1$), and the susceptibility χ [$x_\chi = \nu(2-\eta)$].

The reader may observe that studying g_L rather than g_{2L} in Eq. (16) is somehow arbitrary. In fact, the relative size of scaling corrections cannot be decided a priori.[49] As a rule, we study g_L because its statistical errors are smaller. However, checking that this choice is immaterial will be an important consistency check.

As a general rule, in this work we shall consider only the leading-order corrections to scaling, $O(L^{-\omega})$, that appear in Eq. (16). In some particular cases our statistical errors will be small enough to resolve subleading corrections. We shall represent these subleading corrections in an *effective* way as a second-order polynomial in $L^{-\omega}$. However, corrections of order $L^{-2\omega}$ are only a subclass of the full set of subleading corrections (see, e.g., Ref. 36).

As for the crossing temperature $T_{\rm c}^{(L,2L)}$, we recall that it approaches $T_{\rm c}$ as

$$T_{\rm c}^{(L,2L)} - T_{\rm c} = A L^{-(\omega+1/\nu)} + \dots\,, \qquad (17)$$

where A is a scaling amplitude and the dots stand for subleading corrections.

Finally, we remark that ξ/L in the above outlined analyses could be replaced by any other of the six cumulants, such as for instance U_4.

IV. THE CRITICAL EXPONENTS

Following the quotients method described in the previous section, we could compute all the critical parameters (the critical exponent and the universal values of dimensionless quantities) using fits to (16). For instance, in order to compute the anomalous dimension η we could use the relation

$$Q_\chi^{\rm cross} = 2^{2-\eta} + A_\chi L^{-\omega} + \dots\,. \qquad (18)$$

Hereafter, the dots will stand for subleading corrections to scaling.

In practice, of course, determining both the extrapolated value and the value of the exponent ω in the same fit is very delicate, given the low number of degrees of freedom available. In fact, the usual approach in recent finite-size scaling studies has been to compute ω first, using the behavior of dimensionless quantities, and then use this precomputed value of ω to extrapolate the other critical exponents (see, e.g., Refs. 29 and 48 and also Appendix A). This approach has the disadvantage that all quantities have to be reported with two error bars (the first due to the statistical errors in the fit and the second due to the uncertainty in the precomputed ω). Moreover, it does not take full advantage of the information contained in the critical behavior of quotients of dimensionful quantities (because these are not used to refine the estimate of ω).

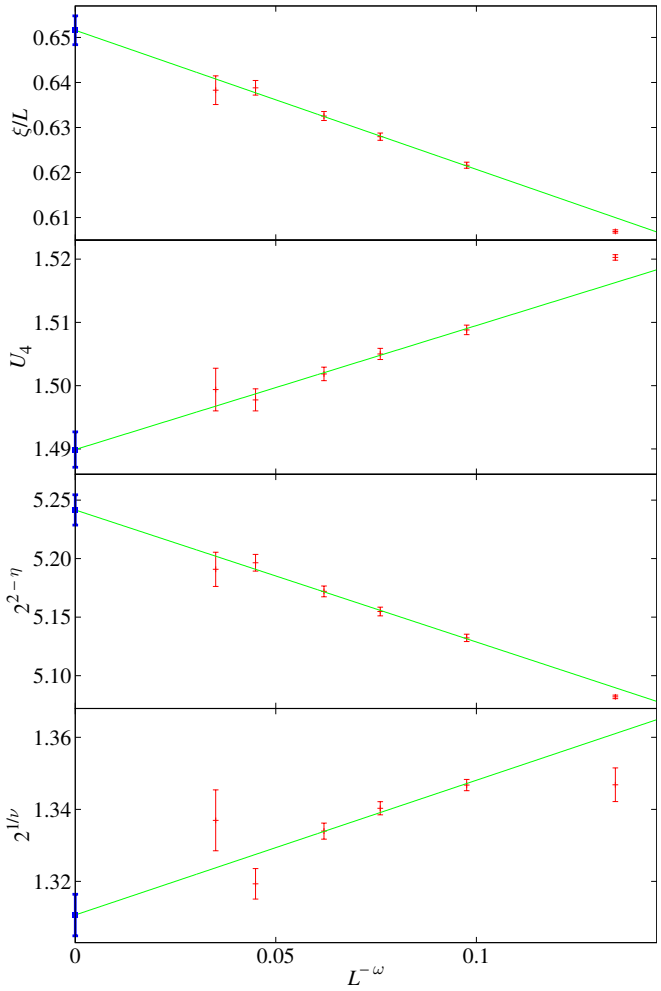

FIG. 2. (color online). Result of a joint fit yielding the critical exponents of the Ising spin glass. As discussed in the text, using the quotients method, we study the approach of two dimensionless universal quantities (U_4 and ξ/L) and of the quotients of two dimensionful quantities (χ and $\partial_T \xi$) to their critical value. The rightmost points (corresponding to the crossings between $L = 6$ and $L = 12$) are not included in the fit. The extrapolated values, reported in Table I, are represented by a thick blue point on the Y axis. The fit, where the same $\omega = 1.12(10)$ is used by the four quantities, has a $\chi^2/\text{d.o.f.} = 13.78/11$. The critical exponents are $\nu = 2.562(42)$, $\eta = -0.3900(36)$.

In this paper, on the other hand, we consider all the most important quantities at the same time in a global fit. In partic-

ular, we take as fitting functions

$$U_4^{\rm cross}(L) = U_4^* + A_{U_4} L^{-\omega}, \tag{19}$$
$$R_\xi^{\rm cross}(L) = R_\xi^* + A_\xi L^{-\omega}, \tag{20}$$
$$Q_\chi^{\rm cross}(L) = 2^{2-\eta} + A_\chi L^{-\omega}, \tag{21}$$
$$Q_{\partial_T \xi/L}^{\rm cross}(L) = 2^{1/\nu} + A_{\partial\xi} L^{-\omega}. \tag{22}$$

Notice that ω is a common parameter in all of these functions. Then, we construct the χ^2 goodness-of-fit estimator as

$$\chi^2 = \sum_{i,j,a,b} [y_i(L_a) - y_i^* - A_i L_a^{-\omega}][\sigma^{-1}]_{(ia)(jb)}[y_j(L_b) - y_j^* - A_j L_b^{-\omega}], \tag{23}$$

where a, b run over the system sizes, L_a denotes the smaller L in each of the crossings $(L, 2L)$, and y_i is any of the $Q_O^{\rm cross}$ or of the $g^{\rm cross}$ of Eqs. (19)–(22). The matrix σ^{-1} is the inverse of the full covariance matrix of the data. This approach is statistically reliable and allows us to extract a large amount of information from the numerical data.

We have plotted this joint fit in Figure 2. We have discarded the data from the $(L, 2L) = (6, 12)$ crossing, which clearly shows subleading corrections to scaling. The resulting fit, with $\chi^2/\text{d.o.f.} = 13.78/11$ ($P = 25\%$) yields the following critical parameters, defining the universality class of the Ising spin glass:

$$\omega = 1.12(10), \quad \eta = -0.3900(36), \quad \nu = 2.562(42), \tag{24}$$

$$R_\xi^* = 0.6516(32), \qquad U_4^* = 1.4899(28). \tag{25}$$

The amplitudes in the fit are

$$\begin{aligned} A_\xi &= -0.309(42), \quad A_{U_4} = 0.196(32), \\ A_\chi &= -0.141(20), \quad A_{\partial\xi} = 0.374(70). \end{aligned} \tag{26}$$

In addition, using the scaling and hyperscaling relations, we can give the value of the remaining critical exponents (taking correlations into account for the errors):

$$\gamma = 6.13(11), \quad \beta = 0.782(10), \quad \alpha = -5.69(13). \tag{27}$$

More generally, for future reference, we report some correlation coefficients (useful to compute the error in derived quantities)

$$r_{\omega\nu} = -0.58, \qquad r_{\omega\eta} = 0.75, \qquad r_{\nu\eta} = -0.76, \tag{28}$$

where

$$r_{AB} = \frac{\text{Cov}(A, B)}{\sqrt{\text{Var}(A)\text{Var}(B)}}\,. \tag{29}$$

We remark that, in principle, we could have added the other dimensionless quantities defined in Section II B to the fit, thus obtaining their values at the critical point as well as presumably improving our determination of ω. The problem, of course, is that there is only so much information in the system. If one keeps adding quantities to the fit, eventually the covariance matrix becomes singular (or, at least, singular for numerical purposes). Therefore, in practice there is a limit to how many different quantities can be analyzed at the same time.

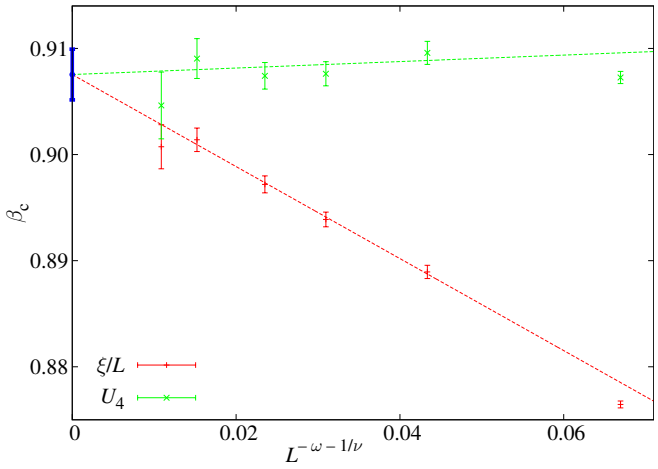

FIG. 3. (color online). Computation of β_c with the quotients method. We fit the crossing point $\beta^{\rm cross}(L)$ of lattices $(L, 2L)$ to $\beta^{\rm cross} = \beta_c + AL^{-\omega-1/\nu}$, using both U_4 and $R_\xi = \xi/L$ to determine $\beta^{\rm cross}$ and discarding the data for the $(6, 12)$ crossing. The common extrapolated value is $\beta_c = 0.9075(11)[\overline{13}]$, where the first error bar is the statistical error in the fit while the second one is due to the error in $\omega + 1/\nu$ (the overline denotes that β_c is anticorrelated with $\omega + 1/\nu$).

Finally, we would like to mention that an alternative way of computing η has been recently suggested.[50] One could compute the spin correlation function in Fourier space, $\chi(\boldsymbol{k})$, conditioned to a fixed value of the spin overlap. In particular $\chi(\boldsymbol{k})|_{q=0}$, where all the thermal averages consider only those pairs of configurations where $|q|$ is smaller than a certain window $q_0 = O(V^{-1/2})$. This has the advantage of reducing the statistical errors significantly with respect to the unrestricted correlation function. However, the fact that we cannot use the $\boldsymbol{k} = 0$ mode introduces stronger corrections to scaling, so we have not followed this alternative approach to compute η (but we have checked that it would give a consistent, though less accurate, estimate).

V. OTHER EXTRAPOLATIONS TO THE THERMODYNAMIC LIMIT

A. The critical temperature

As discussed in Section III, the crossing point behaves as

$$\beta_g^{\rm cross} = \beta_c + A_{\beta_c, g} L^{-\omega-1/\nu} + \ldots, \tag{30}$$

where g denotes the dimensionless quantity used to compute the crossing points.[51] We can use this formula to determine the critical temperature of the system. To this end, we perform a joint fit to Eq. (30) using the crossings computed both with U_4 and with R_ξ (where β_c is a common fit parameter). We take the value of $\omega + 1/\nu$ from the fit in Section IV. The final value,

Universal quantity	$A_{g,\xi}$	A_{g,U_4}	χ^2/d.o.f.
$U^*_{1111} = 0.47141(68)[\overline{70}]$	$-0.0681(87)[\overline{61}]$	0.005(9)[10]	7.72/7
$U^*_{22} = 0.76808(76)[\overline{84}]$	$-0.085(10)[\overline{8}]$	$-0.003(10)[10]$	8.32/7
$U^*_{111} = 0.44886(73)[\overline{77}]$	$-0.0723(93)[\overline{62}]$	0.008(10)[11]	7.86/7
$B^*_\chi = 2.4142(33)[\overline{18}]$	$-0.044(42)[14]$	0.36(4)[10]	8.91/7

TABLE III. Universal quantities at the critical point. We remind the reader that the first error bar is the statistical error in each fit, while the second is the effect of the uncertainty in our estimate of ω (we add an overline if the quantity is anticorrelated with ω). We also give the (non-universal) amplitudes $A_{g,\xi}$ and A_{g,U_4} in the fits.

again fitting for $L \geq 8$ is

$$\beta_c = 0.9075(11)[\overline{13}], \qquad \chi^2/\text{d.o.f.} = 6.15/7. \tag{31}$$

The first error bar is the statistical uncertainty in the fit and the second error bar is due to our uncertainty in $\omega + 1/\nu$. The line over the second error bar denotes that the estimate of β_c is anticorrelated with that of $\omega + 1/\nu$. The corresponding value for T_c is, therefore,

$$T_c = 1.1019(13)[16]. \tag{32}$$

The amplitudes $A_{\beta_c,g}$ are

$$A_{\beta_c,\xi} = -0.434(34)[\overline{58}], \qquad A_{\beta_c,U_4} = 0.031(37)[49]. \tag{33}$$

B. Dimensionless universal quantities

As explained in Section IV, we have not used the non-standard dimensionless ratios defined in Section II B [Eqs. (10)–(14)] to determine the critical exponents of the system. However, since some of these quantities have been found useful in the past[29,37] and since they are universal quantities further characterizing the Ising spin glass universality class, we have found it interesting to report their critical values.

We perform fits to

$$g_L^{\text{cross}} = g^* + A_g L^{-\omega}, \tag{34}$$

where g is each of $U_{1111}, U_{111}, U_{22}, R_{12}$ and B_χ. We take ω from Eq. (24). In all cases we include all data with $L \geq 8$. In order to improve our statistics, we consider for each g its scaling on the crossing point of both U_4 and R_ξ (with common extrapolation g^*). Table III displays the results for all quantities but R_{12}.

In fact, we realized that R_{12} deserves a special analysis when making the consistency test alluded to in Sect. III. We performed again the fit in Eq. (34), but for g_{2L}^{cross} this time. If subdominant scaling corrections are truly negligible, as we assume in Eq. (34), the universal extrapolation g^* must come out compatible. The estimate of g^* changed by less than one tenth of an error bar for U_{1111}, U_{111} and U_{22}. In the case of B^*_χ the obtained result varied a full error bar (we obtained $B^*_\chi = 2.4218(35)[\overline{42}]$ in the fit with g_{2L}). Given the data correlation, this difference might be significant, so we suggest doubling the error for B^*_χ in Table III if one wants to be specially careful.

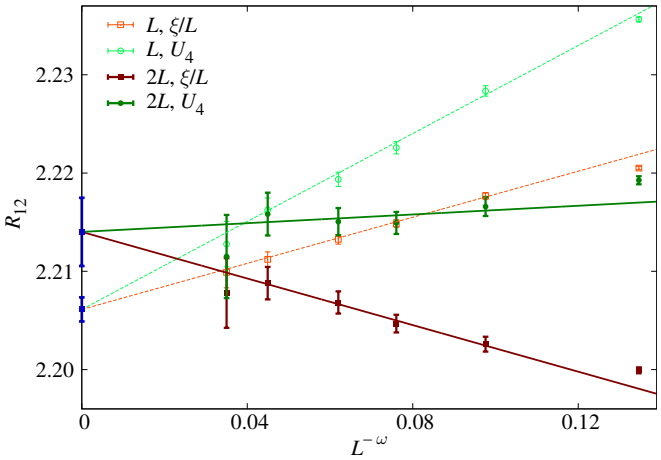

FIG. 4. (color online). Resolving the ambiguity in Eq. (34): at the crossing point of ξ/L or U_4, one is free to consider the dimensionless quantity g as computed for the small system (g_L^{cross}) or for the large system (g_{2L}^{cross}). This choice turns out to be immaterial for all quantities reported in Table III, but not for R_{12}. In the plot, we display the values of R_{12} at the corresponding crossing point, as a function of $L^{-\omega}$. Empty (full) symbols correspond to the small (large) lattice in the pair $(L, 2L)$ involved in the crossing. Lines are fits to Eq. (34), constrained to yield a common extrapolation for the ξ/L crossings and for the U_4 crossings. The dashed (full) lines correspond to the fits for the small (large) lattices. The corresponding extrapolations are depicted in blue on the $L^{-\omega} = 0$ axis. Both fits are performed for $L \geq 8$ and of good statistical quality: $\chi^2/\text{d.o.f.} = 7.0/7$ (small lattice) and $\chi^2/\text{d.o.f.} = 5.9/7$ (large lattice). In spite of this, both extrapolations are incompatible. Our final value for R^*_{12}, Eq. (35), corresponds to the minimal interval that includes both extrapolations and their statistical errors.

Unfortunately, subleading scaling corrections are more difficult to control for R^*_{12}. The extrapolation for g_L and g_{2L} are clearly incompatible, see Figure 4. Considering subleading corrections of order $L^{-2\omega}$ does not improve the situation. Therefore, we have chosen a more conservative approach: we give as a final estimate the interval covering both extrapolations and their errors

$$R^*_{12} = 2.211 \pm 0.006\,. \tag{35}$$

We emphasize that, when comparing with future work, it will be necessary to keep in mind that the error in Eq. (35) is of systematic rather than of statistical nature.

VI. CONCLUSIONS

In this paper we have performed a finite-size scaling study of the critical behavior of the Ising spin glass, using data from large-scale parallel tempering simulations performed on the Janus computer. We have followed a strategy based on the application of the quotients method and on the use of joint

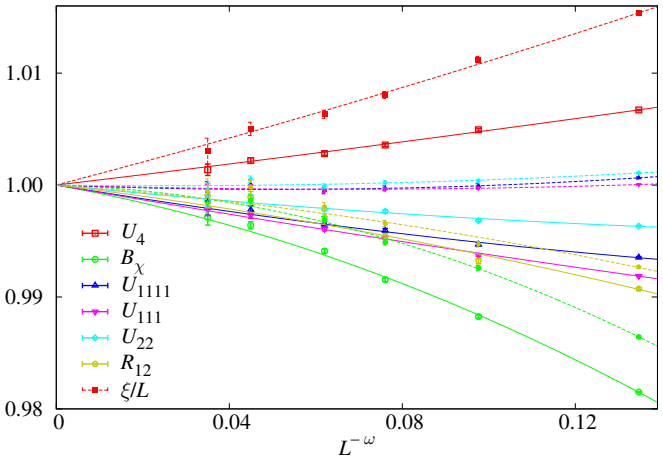

FIG. 5. (color online). Quotients of dimensionless quantities computed at the crossing points of ξ/L (open symbols) and of U_4 (filled symbols). We also plot individual fits to (A1) (solid lines for ξ/L and dotted lines for U_4).

fits of several quantities to obtain accurate estimates of all the critical exponents of the system. We have also computed the critical value of several universal dimensionless quantities, as well as the value of the critical temperature.

ACKNOWLEDGMENTS

The total simulation time devoted to this project was the equivalent of 107 days of the full Janus machine ($L \geq 32$) and 43 days of the full (3072 cores) *Memento* cluster. For information about both machines, see also http://bifi.es.

The Janus project has been partially supported by the EU (FEDER funds, No. UNZA05-33-003, MEC-DGA, Spain); by the European Research Council under the European Union's Seventh Framework Programme (FP7/2007-2013, ERC grant agreement no. 247328); by the MICINN (Spain) (contracts FIS2006-08533, FIS2012-35719-C02, FIS2010-16587, TEC2010-19207); by the SUMA project of INFN (Italy); by the Junta de Extremadura (GR10158); by the Microsoft Prize 2007 and by the European Union (PIRSES-GA-2011-295302). F.R.-T. was supported by the Italian Research Ministry through the FIRB project No. RBFR086NN1; M.B.-J. was supported by the FPU program (Ministerio de Educacion, Spain); R.A.B. and J.M.-G. were supported by the FPI program (Diputacion de Aragon, Spain); finally J.M.G.-N. was supported by the FPI program (Ministerio de Ciencia e Innovacion, Spain).

Appendix A: Alternative computation of exponent ω

As mentioned in section IV, the computation of the scaling corrections exponent ω is the most delicate step in the analysis. Therefore, we present in this appendix an alternative way of approaching it, as a consistency check of our results.

We start by making the rather obvious remark that the quotient $Q_g = g_{2L}/g_L$ of any dimensionless quantity g at the crossing points $\beta^{\rm cross}$ defined by any other dimensionless quantity h [so $h_L(\beta^{\rm cross}) = h_{2L}(\beta_{\rm cross})$] goes to one as the system size increases

$$Q_g^{\rm cross}(L) = 1 + A_g L^{-\omega} + B_g L^{-2\omega} + \ldots , \qquad \text{(A1)}$$

The advantage of this equation is that, unlike in our analysis of Section IV, the asymptotic value is not another parameter in the fit, but known in advance. We show $Q_g^{\rm cross}$ in Figure 5 for $g = U_4, R_\xi, U_{1111}, U_{111}, U_{22}, B_\chi$ and R_{12}. In all cases we compute $Q^{\rm cross}$ at the crossing points of both U_4 and R_ξ (except for these two quantities, which are obviously considered only at each other's crossing points).

In Figure 5 we have performed individual fits to (A1) for each quantity, using the previously computed value of ω, to show that this description is consistent. From the plot we can see that some of the quantities (such as R_{12}) have very clear subleading scaling corrections, but that for others the leading term in (A1) is quite sufficient.

Armed with this qualitative observation, we can do a second fit to (A1), this time leaving ω free and considering several dimensionless quantities at the same time. In particular, in order to avoid the quadratic term, we have considered U_4, R_ξ, U_{1111} and U_{111} and discarded the data for $L = 6$. The result of this joint fit is

$$\omega = 1.187(68), \qquad \chi^2/\text{d.o.f.} = 19.80/23, \qquad \text{(A2)}$$

compatible with our previous determination of ω.

[1] J. A. Mydosh, *Spin Glasses: an Experimental Introduction* (Taylor and Francis, London, 1993).
[2] M. Mézard, G. Parisi, and M. Virasoro, *Spin-Glass Theory and Beyond* (World Scientific, Singapore, 1987).
[3] S. F. Edwards and P. W. Anderson, J. Phys. F **5**, 965 (1975).
[4] M. Palassini and S. Caracciolo, Phys. Rev. Lett. **82**, 5128 (1999), arXiv:cond-mat/9904246.
[5] H. G. Ballesteros, A. Cruz, L. A. Fernandez, V. Martin-Mayor, J. Pech, J. J. Ruiz-Lorenzo, A. Tarancon, P. Tellez, C. L. Ullod, and C. Ungil, Phys. Rev. B **62**, 14237 (2000), arXiv:cond-mat/0006211.
[6] N. Kawashima and A. P. Young, Phys. Rev. B **53**, R484 (1996).
[7] D. Iñiguez, G. Parisi, and J. J. Ruiz-Lorenzo, J. Phys. A: Math. and Gen. **29**, 4337 (1996).
[8] E. Marinari, G. Parisi, and J. J. Ruiz-Lorenzo, Phys. Rev. B **58**, 14852 (1998).
[9] D. Iñiguez, E. Marinari, G. Parisi, and J. J. Ruiz-Lorenzo, J. Phys. A: Math. and Gen. **30**, 7337 (1997).
[10] B. A. Berg and W. Janke, Phys. Rev. Lett. **80**, 4771 (1998).
[11] W. Janke, B. A. Berg, and A. Billoire, Ann. Phys. **7**, 544 (1998).
[12] K. Gunnarsson, P. Svendlindh, P. Nordblad, L. Lundgren, H. Aruga, and A. Ito, Phys. Rev. B **43**, 8199 (1991).

[13] P. O. Mari and I. A. Campbell, Phys. Rev. B **65**, 184409 (2002).
[14] T. Nakamura, S.-i. Endoh, and T. Yamamoto, J. Phys. A **36**, 10895 (2003).
[15] D. Daboul, I. Chang, and A. Aharony, Eur. Phys. J. B **41**, 231 (2004).
[16] M. Pleimling and I. A. Campbell, Phys. Rev. B **72**, 184429 (2005).
[17] S. Perez-Gaviro, J. J. Ruiz-Lorenzo, and A. Tarancón, J. Phys. A: Math. Gen. **39**, 8567 (2006).
[18] F. Parisen Toldin, A. Pelissetto, and E. Vicari, J. Stat. Mech.: Theory Exp. , P06002 (2006).
[19] T. Jörg, Phys. Rev. B **73**, 224431 (2006).
[20] I. A. Campbell, K. Hukushima, and H. Takayama, Phys. Rev. Lett. **97**, 117202 (2006).
[21] H. G. Katzgraber, M. Körner, and A. P. Young, Phys. Rev. B **73**, 224432 (2006).
[22] J. Machta, C. M. Newman, and D. L. Stein, J. Stat. Phys. **130**, 113 (2008).
[23] M. Hasenbusch, A. Pelissetto, and E. Vicari, J. Stat. Mech. , L02001 (2008).
[24] M. Hasenbusch, A. Pelissetto, and E. Vicari, Phys. Rev. B **78**, 214205 (2008).
[25] T. Jörg and H. G. Katzgraber, Phys. Rev. B **77**, 214426 (2008), arXiv:0803.3339.
[26] F. Belletti, M. Cotallo, A. Cruz, L. A. Fernández, A. Gordillo, A. Maiorano, F. Mantovani, E. Marinari, V. Martín-Mayor, A. Muñoz Sudupe, D. Navarro, S. Pérez-Gaviro, J. J. Ruiz-Lorenzo, S. F. Schifano, D. Sciretti, A. Tarancón, R. Tripiccione, and J. L. Velasco (Janus Collaboration), Comp. Phys. Comm. **178**, 208 (2008), arXiv:0704.3573.
[27] F. Belletti, M. Guidetti, A. Maiorano, F. Mantovani, S. F. Schifano, R. Tripiccione, M. Cotallo, S. Perez-Gaviro, D. Sciretti, J. L. Velasco, A. Cruz, D. Navarro, A. Tarancon, L. A. Fernandez, V. Martin-Mayor, A. Muñoz-Sudupe, D. Yllanes, A. Gordillo-Guerrero, J. J. Ruiz-Lorenzo, E. Marinari, G. Parisi, M. Rossi, and G. Zanier (Janus Collaboration), Computing in Science and Engineering **11**, 48 (2009).
[28] R. Alvarez Baños, A. Cruz, L. A. Fernandez, J. M. Gil-Narvion, A. Gordillo-Guerrero, M. Guidetti, A. Maiorano, F. Mantovani, E. Marinari, V. Martin-Mayor, J. Monforte-Garcia, A. Muñoz Sudupe, D. Navarro, G. Parisi, S. Perez-Gaviro, J. J. Ruiz-Lorenzo, S. F. Schifano, B. Seoane, A. Tarancon, R. Tripiccione, and D. Yllanes (Janus Collaboration), Phys. Rev. Lett. **105**, 177202 (2010), arXiv:1003.2943.
[29] R. A. Baños, A. Cruz, L. A. Fernandez, J. M. Gil-Narvion, A. Gordillo-Guerrero, M. Guidetti, D. Iniguez, A. Maiorano, E. Marinari, V. Martin-Mayor, J. Monforte-Garcia, A. Muñoz Sudupe, D. Navarro, G. Parisi, S. Perez-Gaviro, J. J. Ruiz-Lorenzo, S. F. Schifano, B. Seoane, A. Tarancon, P. Tellez, R. Tripiccione, and D. Yllanes, Proc. Natl. Acad. Sci. USA **109**, 6452 (2012).
[30] M. Baity-Jesi, R. A. Baños, A. Cruz, L. A. Fernandez, J. M. Gil-Narvion, A. Gordillo-Guerrero, D. Iniguez, A. Maiorano, M. F., E. Marinari, V. Martin-Mayor, J. Monforte-Garcia, A. Muñoz Sudupe, D. Navarro, G. Parisi, S. Perez-Gaviro, M. Pivanti, F. Ricci-Tersenghi, J. J. Ruiz-Lorenzo, S. F. Schifano, B. Seoane, A. Tarancon, R. Tripiccione, and D. Yllanes, (2013), arXiv:1307.4998.
[31] K. Hukushima and K. Nemoto, J. Phys. Soc. Japan **65**, 1604 (1996), arXiv:cond-mat/9512035.
[32] E. Marinari, in *Advances in Computer Simulation*, edited by J. Kerstész and I. Kondor (Springer-Berlag, 1998).
[33] R. Alvarez Baños, A. Cruz, L. A. Fernandez, J. M. Gil-Narvion, A. Gordillo-Guerrero, M. Guidetti, A. Maiorano, F. Mantovani, E. Marinari, V. Martin-Mayor, J. Monforte-Garcia, A. Muñoz Sudupe, D. Navarro, G. Parisi, S. Perez-Gaviro, J. J. Ruiz-Lorenzo, S. F. Schifano, B. Seoane, A. Tarancon, R. Tripiccione, and D. Yllanes (Janus Collaboration), J. Stat. Mech. , P06026 (2010), arXiv:1003.2569.
[34] L. A. Fernandez, A. Maiorano, E. Marinari, V. Martin-Mayor, D. Navarro, D. Sciretti, A. Tarancon, and J. L. Velasco, Phys. Rev. B **77**, 104432 (2008), arXiv:0710.4246.
[35] F. Cooper, B. Freedman, and D. Preston, Nucl. Phys. B **210**, 210 (1982).
[36] D. J. Amit and V. Martin-Mayor, *Field Theory, the Renormalization Group and Critical Phenomena*, 3rd ed. (World Scientific, Singapore, 2005).
[37] A. Billoire, L. A. Fernandez, A. Maiorano, E. Marinari, V. Martin-Mayor, and D. Yllanes, J. Stat. Mech. , P10019 (2011), arXiv:1108.1336.
[38] M. P. Nightingale, Physica A **83**, 561 (1975).
[39] H. G. Ballesteros, L. A. Fernandez, V. Martin-Mayor, and A. Muñoz Sudupe, Phys. Lett. B **378**, 207 (1996), arXiv:hep-lat/9511003.
[40] H. G. Ballesteros, L. A. Fernandez, V. Martin-Mayor, A. Muñoz Sudupe, G. Parisi, and J. J. Ruiz-Lorenzo, Phys. Rev. B **58**, 2740 (1998).
[41] I. Campos, M. Cotallo-Aban, V. Martin-Mayor, S. Perez-Gaviro, and A. Tarancon, Phys. Rev. Lett. **97**, 217204 (2006).
[42] L. A. Fernandez, V. Martin-Mayor, S. Perez-Gaviro, A. Tarancon, and A. P. Young, Phys. Rev. B **80**, 024422 (2009).
[43] L. Leuzzi, G. Parisi, F. Ricci-Tersenghi, and J. J. Ruiz-Lorenzo, Phys. Rev. Lett. **101**, 107203 (2008).
[44] R. A. Baños, L. A. Fernandez, V. Martin-Mayor, and A. P. Young, Phys. Rev. B **86**, 134416 (2012), arXiv:1207.7014.
[45] M. Baity-Jesi, L. A. Fernandez, V. Martin-Mayor, and J. M. Sanz, (2013), arXiv:1309.1599.
[46] L. A. Fernandez, V. Martin-Mayor, and D. Yllanes, Phys. Rev. B **84**, 100408(R) (2011), arXiv:1106.1555.
[47] L. A. Fernandez, A. Gordillo-Guerrero, V. Martin-Mayor, and J. J. Ruiz-Lorenzo, Phys. Rev. B **86**, 184428 (2012), arXiv:1205.0247.
[48] N. G. Fytas and V. Martin-Mayor, Phys. Rev. Lett. **110**, 227201 (2013), arXiv:1304.0318.

[49] Dimensionless quantities behave as a function of L and the reduced temperature $t = (T - T_c)/T_c$ as

$$g(L,t) = f_g(L^{1/\nu}t) + L^{-\omega}h_g(L^{1/\nu}t) + \dots ,$$

where f_g and h_g are very smooth (actually analytical) scaling functions. In particular, we name f_ξ and g_ξ the scaling functions corresponding to ξ/L. In fact, see e.g. Ref. 36, the detailed form of Eq. (17) follows from the Taylor expansions $f_\xi(x) = f_\xi(0) + x f'_\xi(0) + \dots$ and $h_\xi(x) = h_\xi(0) + \dots$:

$$t^{\rm cross}_{L,2L} = \frac{h_\xi(0)}{f'_\xi(0)} \frac{1-2^{-\omega}}{2^{1/\nu}-1} L^{-\omega-\frac{1}{\nu}} + \dots .$$

A similar computation yields the amplitudes for the scaling corrections of $g^{\rm cross}_{2L}$ and $g^{\rm cross}_{L}$ in Eq. (16):

$$A^{(2L)}_g = 2^{1/\nu}\frac{1-2^{-\omega}}{2^{1/\nu}-1} h_\xi(0)\frac{f'_g(0)}{f'_\xi(0)} + 2^{-\omega}h_g(0) ,$$

and

$$A^{(L)}_g = \frac{1-2^{-\omega}}{2^{1/\nu}-1} h_\xi(0)\frac{f'_g(0)}{f'_\xi(0)} + h_g(0)$$

Either of the two amplitudes $A^{(L)}_g$, $A^{(2L)}_g$ can dominate, depending both on g and on the magnitude chosen to find the crossing point (ξ/L, U_4, etc.).

[50] D. Yllanes, *Rugged Free-Energy Landscapes in Disordered Spin Systems* (Ph.D. thesis, UCM, 2011) arXiv:1111.0266.

[51] As usual, $\beta = 1/T$. We employ it in order to allow for a direct comparison with raw data from Ref. 24.